Polymer 51 (2010) 4095–4102

Contents lists available at ScienceDirect

Polymer

journal homepage: www.elsevier.com/locate/polymer

Self-assembly of cationic rod-like poly(2,5-pyridine) by acidic bis(trifluoromethane)-sulfonimide in the hydrated state: A highly-ordered self-assembled protonic conductor

M. Vilkman [a,b,*], A. Lankinen [c], N. Volk [a], P. Kostamo [c], O. Ikkala [a]

[a] Aalto University School of Science and Technology (previously Helsinki University of Technology), Molecular Materials, P.O. Box 15100, FI-00076, Espoo, Finland
[b] VTT Technical Research Centre of Finland, Printed Functional Solutions, P.O. Box 1000, FI-02044 VTT, Finland
[c] Aalto University School of Science and Technology (previously Helsinki University of Technology), Department of Micro- and Nanosciences, P.O. Box 13500, FI-00076 Aalto, Espoo, Finland

ARTICLE INFO

Article history:
Received 10 April 2010
Received in revised form
27 June 2010
Accepted 2 July 2010
Available online 30 July 2010

Keywords:
Poly(2,5-pyridine)
Self-assembly
Ionic liquid anion

ABSTRACT

We show that acid–base complexation of rod-like poly(2,5-pyridine) (PPY) by bis(trifluoromethane) sulfonimide (TFSI) leads to highly-ordered lamellar self-assemblies in the hydrated films and shows relatively high room temperature conductivity of ca. 10^{-4} S/cm. Thin films with different nominal degrees of complexation were studied using X-ray diffraction, Fourier transform infrared spectroscopy, contact angle measurements, conductivity measurements, and polarised optical microscopy. We propose that the self-assembly is promoted by the amphiphilicity of TFSI and the interplay between the hydrophilic and hydrophobic sites within the complexes. The hydrophilic sites allow confinement of water molecules within the hydrated self-assemblies for low loading of TFSI to promote proton conductivity. For high loading of TFSI in the hydrated state, another coincident self-assembled structure is additionally observed, which we suggest to form due to phase separated water/TFSI domains, as resembling lamellar water/surfactant liquid crystalline phases. The new type of self-assembled acid–base material combining rod-like polymeric cations and ionic liquid anions suggests new routes for ionic and protonic transport and functional materials.

1. Introduction

The structural organisations within different conducting polymers have strong effects on the functionality and transport properties. For example, in conjugated polymers a well defined self-assembly results in high charge-carrier mobility in polythiophene-based field-effect transistors [1–4]. Self-assembly allows also feasible transport properties in lithium-conducting ionic conductors as pursued e.g. for the next generation batteries [5,6]. As relevant for the present work, structural control and percolating water networks are needed in proton-conducting polymers *e.g.* for fuel cells (for comprehensive present view see refs [7,8]). They have been studied extensively in perfluorinated sulfonic acid membranes, like Nafion®, which enable high conductivity and anomalous proton mobility due to percolative aqueous networks based on competition of hydrophobicity due to the fluorines and hygroscopicity due to the sulfonic acid anions [9–12]. There have been a multitude of efforts towards providing alternatives for Nafions, in an effort to provide rationally designed percolative water channels and transport properties by self-assembly [13–20]. Self-assembled water domains have been pursued using comb-shaped architectures without fluorination [21] and with fluorination [22] using sulphonic acids as the hygroscopic groups. Also nonfluorinated aromatic compositions with sulphonic acids have been explored, as well as acid–base salts [23].

Another approach towards protonically conducting compositions has been explored based on ionic liquids in an effort to find materials that could even work under less hydrated conditions [24]. Therein bis(trifluoromethane)sulfonimide (TFSI) has been explored, as it is one of the strongest superacids, having a delocalised negative charge on the nitrogen and oxygen atoms within the acid anion [25–34]. High protonic conductivity has been observed in several salts with organic oligomers, such as imidazole, substituted imidazoles, benzimidazole, oxazole, and alkyl viologen [35–39]. Transport within salts with cationic polymers has been

* Corresponding author at: VTT Technical Research Centre of Finland, Printed Functional Solutions, P.O.Box 1000, FI-02044 VTT, Finland. Tel.: +358 20 722 7132; fax: +358 20 722 7012.
E-mail address: marja.vilkman@vtt.fi (M. Vilkman).

0032-3861/$ – see front matter © 2010 Elsevier Ltd. All rights reserved.
doi:10.1016/j.polymer.2010.07.005

explored based on linear polyethylene imines, poly(*p*-phenylene-2,5-(1,3,4-oxadiazole)), and amine-containing rigid polymers [40–42].

In this work, we investigate self-assemblies of complexes based on acidic TFSI and rigid rod polymeric cations, as encouraged by several reasons. First, it is conceptually interesting whether sufficient plasticisation of rigid rod polymers could be achieved by acid–base complexation with TFSI to allow self-assembly or liquid crystallinity. Note that recently self-assemblies have been demonstrated by mixing block copolymers with ionic liquid salts, such as mixing poly(styrene)-*block*-poly(ethylene oxide) (PS-PEO) with 1-ethyl-3-methylimidazolium bis(trifluoromethylsulfonyl)imide or poly(styrene-*block*-2-vinylpyridine) with an imidazolium bis(trifluoromethane)sulphonamide [43–45]. Such concepts differ from the present case, as the block copolymer does not form a component within the salt. Also, complexes of rigid rod polymers with TFSI have been explored, but the self-assemblies and structures have not been addressed [40,42]. Secondly, the self-assemblies could allow routes towards well defined protonic transport and water channels. In this study, we used poly(2,5-pyridine) (PPY) as a model rod-like heteroaromatic basic polymer to which strongly acidic TFSI is expected to form an acid–base complex (see Fig. 1 for the components). TFSI has an amphiphilic character, *i.e.* it contains very hydrophobic peripheral parts due to multiple fluorine atoms; however, the acidic sulfonimide group is highly hydrophilic [46]. Previously it has been observed that PPY complexes with surfactants have a strong tendency for self-assemblies [47–49]. Therefore we expected that also the complexes with TFSI could self-assemble, as the fluorines lead to highly hydrophobic peripheral patches along the PPY(TFSI) chains, whereas the pyridinium sulfonimides form polar domains. Such a competition between interactions was also expected to lead to compartmentalized water channels along the PPY chains. The potential feasibility was further supported by the previous results, as the TFSI anions are known to allow ionic liquids, which are good protonic conductors having large water uptake when incorporated in a rigid rod elastomeric polymer matrix [42].

The properties of PPY(TFSI)$_x$ thin films were studied with X-ray diffraction (XRD), Fourier transform infrared (FT-IR) spectroscopy, conductivity measurements, contact angle measurements, and polarised optical microscopy.

2. Experimental

Poly(2,5-pyridine) (molecular weight 4000 g/mol) was purchased from Polymer Source Inc. and purified with the following procedure. First PPY was dissolved in methane sulfonic acid (MSA) (10 wt.%), and the mixture was stirred for 2 days to dissolve the polymer completely. Then the PPY-MSA solution was slowly added to a large amount of water that was stirred simultaneously. After mixing the PPY-MSA solution and water, PPY precipitated from the solution. The solution was left to stand still for 1 day and the precipitate was separated from the solution with a centrifuge. The solid material was washed several times with water until the washing solution remained uncoloured. The centrifugation was repeated after each cycle. The purified polymer was then dried on a hot plate at 60 °C and subsequently in vacuum for three days. The colour of the polymer changed from brownish to bright orange after the purification treatment. The drawback of the purification process is that a small amount of residual MSA remains attached to the PPY chain by ionic bonds. However, since we washed the complex several times with water, and Fourier transform infrared spectroscopy of purified PPY showed no signs of protonation, we may assume that the amount of MSA in the complex is low. The purity of the polymer was checked with Energy Dispersive X-ray Fluorescence (EDXRF) at Oxford Instruments Analytical and the amount of metallic impurities (mainly nickel) decreased significantly, and Ni was found to be present ca. 4000 ppm in the purified polymer. The amount of sulphur, arising from the residual MSA, was ca. 1% but it was not possible to measure the exact amount since the light elements (hydrogen and carbon) are not directly detected by the instrument. PPY was dissolved in formic acid and filtered through a 1 μm filter after the purification process.

Li-TFSI was purchased from Aldrich and it was used without purification. The lithium salt form was weighted and stored in a nitrogen glove box in order to avoid water absorption and dissolved afterwards in formic acid. Li-TFSI was converted to the acidic HTFSI with a Dowex Marathon C cation-exchange resin (Aldrich). PPY(TFSI)$_x$ complexes were prepared in the formic acid solution right after the ion exchange reaction.

X-ray diffraction (XRD) curves were measured with a Philips X'Pert Pro MRD diffractometer utilising Cu Kα radiation. The X-ray optics utilised in the measurements consisted of a programmable divergence slit, a Ni filter and a Soller slit on the incident beam side and a programmable receiving slit, a programmable anti scatter slit, and a diffracted beam graphite monocromator on the diffracted beam side. In the diffraction curves, θ is the scattering angle, *i.e.* the Bragg angle, and ω is the angle between the incident beam and the sample surface. In the XRD measurements θ was kept equal to ω and thus the diffraction data was obtained from the crystallographic planes parallel to the sample surface. Consequently, crystallographic planes that are not parallel to the sample surface did not produce any measurable diffraction intensity.

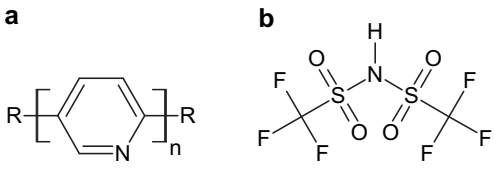

Fig. 1. Molecular formulae of a) poly(2,5-pyridine) (PPY) and b) bis(trifluoromethane) sulfonimide (TFSI).

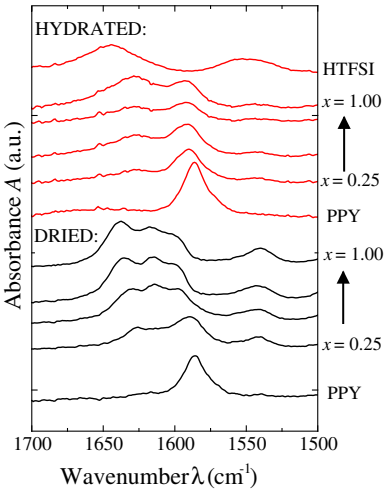

Fig. 2. ATR spectra of PPY, TFSI and PPY(TFSI)$_x$ samples right after vacuum drying (black curves), and after hydration at 80% RH for 150 h (red curves) for 1700–1500 cm^{-1}. The nominal degree of complexation x is indicated. (For interpretation of the references to colour in this figure legend, the reader is referred to the web version of this article).

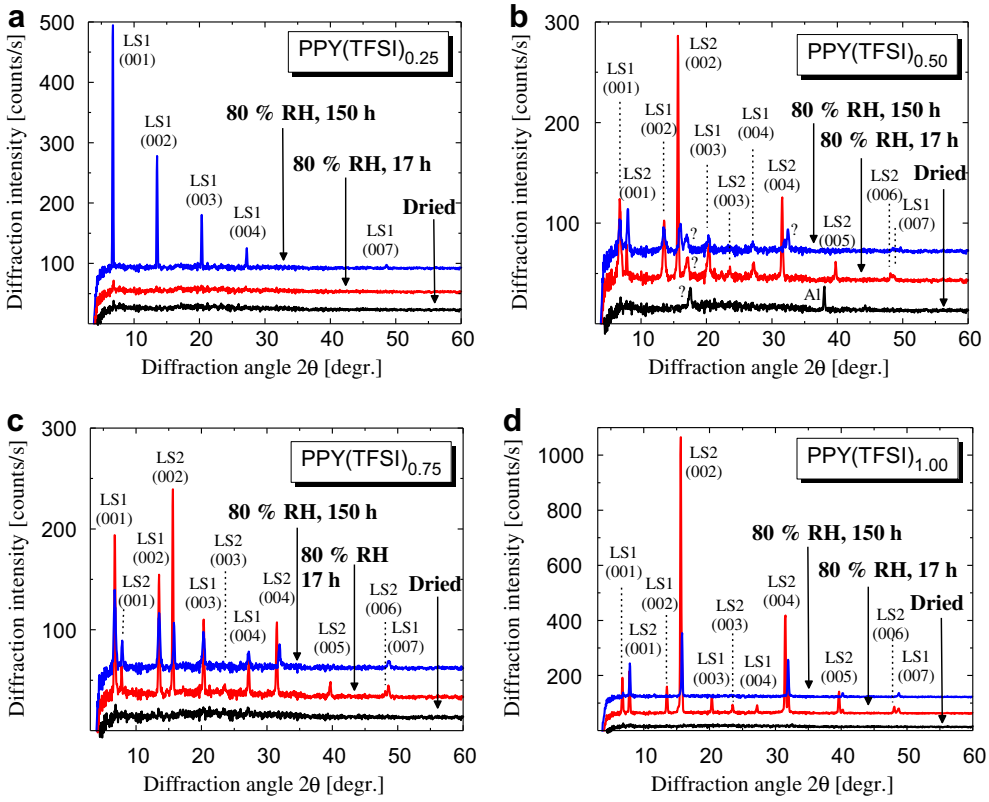

Fig. 3. $2\theta/\omega$ XRD curves of a) $PPY(TFSI)_{0.25}$, b) $PPY(TFSI)_{0.50}$, c) $PPY(TFSI)_{0.75}$ and d) $PPY(TFSI)_{1.00}$ stored in a dry atmosphere after deposition (black curve), after a short 17 h water vapour treatment (red curve), and after a long 150 h water vapour treatment (blue curve) at humidity 80% RH. LS1 (lattice structure I) and LS2 (lattice structure II) denote the two distinct periodic structures having lattice constants of 13.08 Å and 11.31 Å, respectively. Also, aluminium peaks (originating from the substrate holder) and unknown peaks are denoted with Al and a question mark, respectively. (For interpretation of the references to colour in this figure legend, the reader is referred to the web version of this article).

Fourier transform infrared (FT-IR) spectra were obtained using a Nicolet 380 FT-IR spectrometer with an Attenuated Total Reflection (ATR) setup. A minimum of 64 scans were averaged at a resolution of 2 cm^{-1}. The spectra were recorded from spin-coated films on microscope glass slides. The same samples were used to measure the XRD curves.

The optical microscopy pictures were taken with a digital camera (Leica DSC 420) connected to an optical microscope (Leica DM 4500 P) utilising the crossed polariser setup.

Conductivity of the complexes was measured from drop cast samples with a Keithley 2400 Sourcemeter. The samples were prepared from a formic acid solution on cup-shaped glass substrates having four evaporated gold electrodes on the surface with a spacing of 1 mm. The resistance of the films was determined with a four-probe method, where we applied a sequence of currents (+100 nA, −100 nA, +50 nA, −50 nA and 0 nA) to the electrodes, and measured the resulting voltage. Each current was applied for 20 times. This way it was possible to find out whether the conductivity had more of an ionic or electronic character. The resistance was calculated using the voltage value measured at the 20th point at +/− 100 nA and it was converted to the conductivity value by using an estimated average thickness value

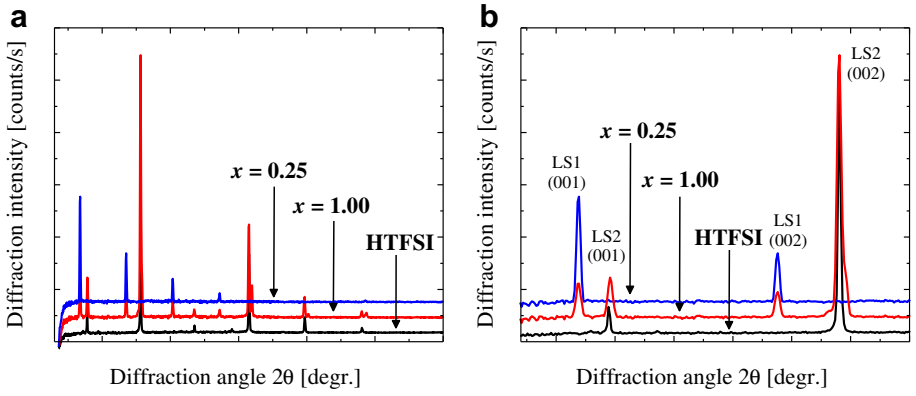

Fig. 4. $2\theta/\omega$ XRD curves of $PPY(TFSI)_{0.25}$ after 150 h at 80% RH humidity (blue curve), $PPY(TFSI)_{1.00}$ after 17 h at 80% RH humidity (red curve), and HTFSI after 17 h at 80% RH humidity (black curve) a) for the whole diffraction angle range and b) showing a magnified range for the first two peaks. LS1 and LS2 denote the two distinct lattice structures having lattice constants of 13.08 Å and 11.31 Å, respectively. (For interpretation of the references to colour in this figure legend, the reader is referred to the web version of this article).

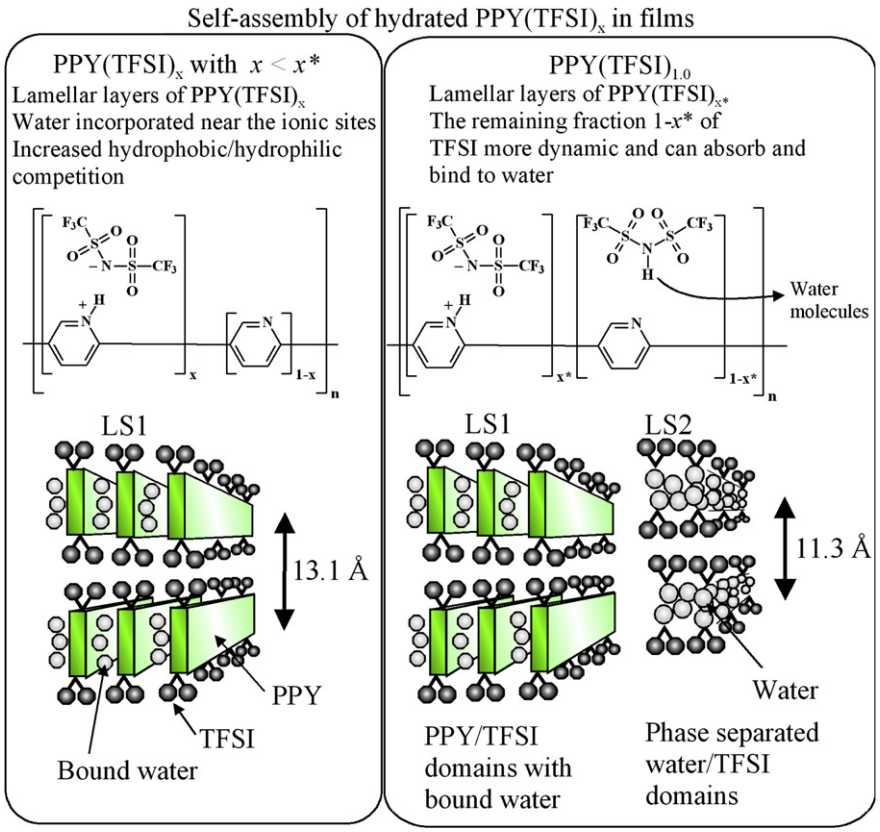

Fig. 5. The suggested schematic presentation of PPY(TFSI) in the hydrated state in thin films on a glass substrate. For low nominal degrees of complexation (up to a limiting value x^* which is between 0.25 and 0.50), there is only lamellar self-assembly due to PPY/TFSI complexes incorporating absorbed water within the structure. For higher nominal degrees of complexation, the added TFSI further increases the hygroscopicity to cause phase separation of additional water which binds with the highly acidic amphiphilic TFSI molecules.

(based on the weight of the sample). The samples were measured as dry, *i.e.* immediately after the removal from vacuum, and after a controlled humidity treatment at 80% RH and 25 °C for one week.

The contact angles of water droplets on spin-coated PPY, PPY(TFSI) and HTFSI films on glass where measured with CAM200 (KSV Instruments Ltd.). The data were measured at 40% RH for dried and humidity treated samples (150 h, 80% RH). The dried films were kept in a desiccator after drying in vacuum and they were exposed to humid air only during the measurement.

All of the experiments were performed for dry and hydrated films. The humidity treatment of the films was done in an environmental chamber (Espec), where both the humidity and temperature could be controlled. The humidity level was kept at 80% RH and the temperature at 25 °C in every treatment.

3. Results and discussion

TFSI is known to be strongly hygroscopic, but simultaneously having highly hydrophobic character due to several fluorines [46]. As water uptake can be important to both the structures and properties, the materials are studied both in the dried state (glove box conditions $H_2O < 1$ ppm and drying) and after humidification (80% RH and 25 °C using two time periods). TFSI is a strong acid and PPY a polymeric base, and therefore their ionic interaction due to proton transfer would be expected. The complexations using different nominal degrees of complexation x (number of TFSI molecules *vs.* pyridine repeat unit of PPY) are investigated. The complexation takes place, and qualitatively manifests even visually as the hard PPY films become plasticised upon adding TFSI, which also promotes water uptake. As the amount of TFSI reaches the nominally complete complexation, $x = 1.00$, a waxy material is formed in the hydrated state. This becomes as no surprise based on previous studies on complexes with some other cations [25–34], where TFSI efficiently decreases the melting point of the salt to allow ionic liquids. The present qualitative observation suggests that even in the case of rod-like polymeric counter-ions, efficient plasticisation towards low temperature softening takes place. FT-IR allows more detailed investigations for the interactions between PPY and TFSI. The pyridine stretching bands near 1600 cm^{-1} are characteristic to learn how the pyridine nitrogen accepts protonation or hydrogen bonds, and it has been amply studied in polyvinylpyridines [50–52]. Therein the pyridine band near 1600 cm^{-1} undergoes a large shift of ca. 40 cm^{-1} due to protonation by strong acids and a small shift of 4–8 cm^{-1} due to hydrogen bonds. Similarly, in PPY the uncomplexed pyridine has a band near 1586 cm^{-1} (Fig. 2) and in the dried state this band undergoes an up-shift upon adding TFSI, until ultimately for $x = 1.0$ it is observed at 1600 cm^{-1}. The up-shift is probably due to partly delocalised charge in the PPY backbone. But importantly, new bands are simultaneously formed at higher wavenumbers, suggesting partial complexation. There are, however, several absorption peaks making the analysis challenging. For $x = 0.25$, a band at 1626 cm^{-1} is observed, and the large shift suggests that a small amount of added TFSI protonates the pyridines of PPY. This would not be surprising due to the very strong acidity of TFSI. But one observes promoted absorption also at smaller shifts, near 1615 cm^{-1}. For increasing x, the large shift to 1630–1640 cm^{-1} becomes even more distinct, indicating considerable degree of protonation. However, also smaller shifts to ca. 1615 cm^{-1} are observed, suggesting that at higher nominal degrees of complexation some of the TFSI molecules interact with PPY

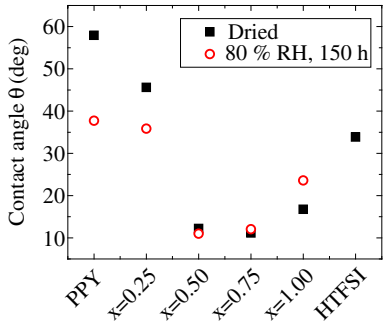

Fig. 6. Water contact angles on pure PPY, PPY(TFSI)$_x$ complexes and pure HTFSI, all spin-coated from formic acid solutions, presented for dried films (black squares) and humidified films (red circles). (For interpretation of the references to colour in this figure legend, the reader is referred to the web version of this article).

based on weaker bonding, *i.e.* hydrogen bonding, beyond protonation. And importantly, a considerable fraction of pyridines remain even uncomplexed, as indicated by the large residual absorption near 1600 cm^{-1}. Therefore we suggest that in the dry state for small degrees of complexation, TFSI binds to PPY mostly due to protonation. Whereas at higher x, the steric crowding hinders complete proton transfer of all the TFSI molecules and part of the TFSI molecules are complexed using weaker hydrogen bonding. It could also be expected that the charge delocalisation within the PPY could pose limitations of how large fraction of TFSI can interact with PPY based on protonation. However, quantitative determination of the actual degrees of absorption based on these FT-IR bands could not be done, due to the unknown absorption coefficients.

Water uptake modifies the interaction considerably, see Fig. 2. Also in this case, an up-shift of the pyridine 1586 cm^{-1} band of PPY is observed in the PPY(TFSI)x spectra, until absorption at 1592 cm^{-1} is observed for $x = 1.00$. Upon adding TFSI, another band is observed near 1626 cm^{-1} and its intensity increases as a function of x. The shift is relatively large, suggesting protonation, but it is still smaller than in the dried state. As the hygroscopic TFSI and its salts are known to allow considerable water uptake, the bound water must be located near the protonation site between TFSI and PPY. Therefore we suggest that the lower wavenumber for the hydrated state is caused by water molecules interfering the complexation. This interpretation is also supported by the assumption that the negative charge in the TFSI anion is delocalised over five atoms, which results in a weak coordinating power [53]. In the following, the complexes are denoted as PPY(TFSI)$_x$ according to their nominal degree of complexation x.

In order to explore whether self-assemblies take place, Fig. 3 shows $2\theta/\omega$ XRD curves recorded from PPY(TFSI)$_x$ thin films for different nominal degrees of complexation x. The three different XRD curves correspond to the same samples in a dried state (spin-coated in a nitrogen glove box and dried in vacuum), and in hydrated states after short and long water vapour treatments. In the short water vapour treatment the samples were kept 17 h in an 80% RH atmosphere at 25 °C, whereas in the long water vapour treatment the time was about 150 h.

The XRD curve of PPY(TFSI)$_{0.25}$ film shows several equally spaced sharp peaks (Fig. 3a) upon long humidity treatment, indicating that after water uptake PPY(TFSI)$_{0.25}$ forms a particularly highly-ordered self-assembled lamellar structure with a lattice constant of 13.08 Å. The observed lattice planes are quite accurately parallel to the substrate surface, and the diffraction peaks are very sharp with a 2θ FWHM of about 0.1°, which is quite remarkable for self-assembled polymeric thin films. The observed 13.08 Å self-assembled structure has been denoted by LS1 (lattice structure I), and rather surprisingly even the 7th order Bragg peak is visible in the XRD curve. Shorter humidity treatment shows only very small reflections (Fig. 3a) and the dried film shows no clear reflections. Therefore, the self-assembly is promoted by water uptake. We suggest formation of a self-assembled layered structure, schematically shown in Fig. 5 (left), and two potential reasons for this phenomenon: First, the absorbed water molecules soften the PPY(TFSI)$_{0.25}$ films, and thus promote the achievement of a well ordered state after the quick structure formation in the spin-coating processing step. Another potential reason could be that the absorbed water increases the hydrophilicity near the ionic sites, thus increasing the difference towards the hydrophobic fluorine domains, producing a driving force for the self-assembly.

Fig. 3b shows the XRD curves for PPY(TFSI)$_{0.50}$. Upon extended humidity treatment, equally spaced set of reflections are observed at the same angles as in PPY(TFSI)$_{0.25}$, and the corresponding self-assembly is also here denoted as LS1 and shown in Fig. 5 (left). The reflections are, however, not as sharp as for the hydrated case for $x = 0.25$. But interestingly, Fig. 3b shows that there exists another set of equally spaced reflections, having a lattice constant of 11.31 Å. This structure is denoted as LS2 (lattice structure II). In the dried samples, no clear reflections are observed. Fig. 3c and d indicate qualitatively similar observations for $x = 0.75$ and $x = 1.00$. Both of the structures LS1 and LS2 are observed to appear already after a short water vapour treatment in all of the samples with $0.5 \leq x \leq 1.0$, which would not be surprising as increasing the TFSI content increases the amount of water absorbed within the films. However, none of the XRD peaks corresponding to LS1 in Fig. 3b–d are as sharp or as intense as the ones in Fig. 3a. Thus, while increasing the TFSI content clearly helps the LS1 assembly, it also seems to reduce the state of the self-assembly, or at least the amount of the alignment parallel to the substrate. In the extreme case of PPY(TFSI)$_{1.00}$, the LS1 peaks fully disappear after the long humidity treatment.

Fig. 4 sheds light towards the LS2 peaks. In Fig. 4a, the red curve in the middle shows the scattering pattern of PPY(TFSI)$_{1.00}$ upon

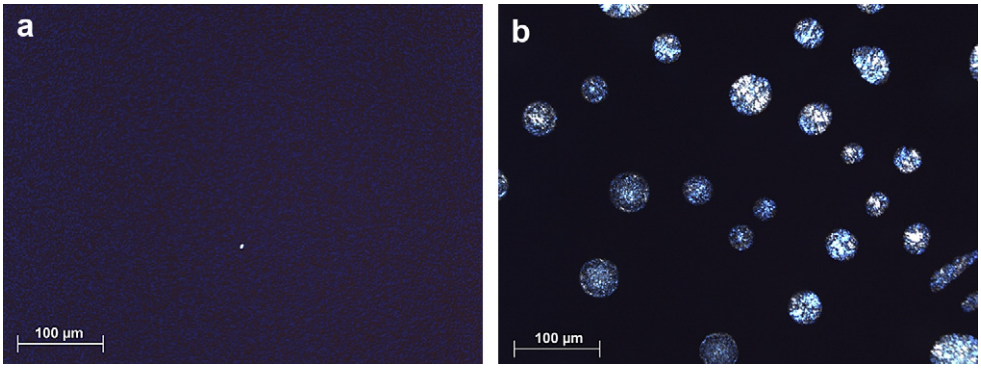

Fig. 7. Polarised optical microscopy pictures of a) PPY(TFSI)$_{0.25}$ and b) PPY(TFSI)$_{1.00}$ films after a humidity treatment of 1 week at 80% RH.

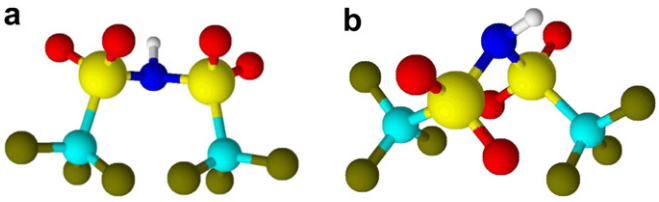

Fig. 8. The conformations a) C_1 and b) C_2 of the TFSI molecule.

a short humidification step. It shows both the LS1 structure and the LS2 structure. Fig. 4b shows a close-up for the scattering angles between 5 and 18°. The blue top curve shows the scattering pattern for PPY(TFSI)$_{0.25}$ after the long humidity treatment, and it shows solely the lamellar self-assembly LS1 between PPY and TFSI (Fig. 5, left). The black bottom curve shows drop cast HTFSI from formic acid without PPY, dried in vacuum and again treated with humid air (80% RH, 25 °C) for water uptake. It forms quite accurately the same LS2 structure as the hydrated PPY(TFSI)$_{1.00}$, which is also observed for all hydrated PPY(TFSI)$_x$ having $x \geq 0.50$. This suggests to assign the LS2 structure to water/TFSI.

Thus a natural interpretation for the reflections in the XRD curves is schematically suggested in Fig. 5: Under dried conditions, no clear signs of self-assemblies were observed in any of the present spin-coated films, whereas upon water uptake self-assemblies are observed. For small nominal degrees of complexation, such as PPY(TFSI)$_{0.25}$, the complexes pack as well defined lamellar self-assemblies with a periodicity of 13.08 Å (LS1 structure) where the low surface energy fluorines are expected to be towards the film surface. This is supported as the moderately high water contact angle of 35°, even if TFSI is very hygroscopic, see Fig. 6. PPY(TFSI)$_{0.25}$ is homogeneous in optical microscopy at all conditions, and does not indicate phase separation of water-rich domains even upon hydration. We suggest that water is absorbed within the self-assembled structure, most probably near the hydrophilic protonation sites between the PPY and TFSI components. Upon adding more hygroscopic TFSI, also more water can be absorbed, which ultimately may lead to phase separation as water-rich domains from the water poor (and PPY-rich) domains. Therefore for $x = 0.50–0.75$, a two-phase structure is observed: In one phase, self-assembled lamellar layers are observed (similar as in PPY(TFS)$_{0.25}$) as manifested in XRD in the highly-ordered LS1 lamellar self-assembly with the periodicity of 13.08 Å, see Fig. 5 for the scheme. But FT-IR qualitatively shows that a considerable amount of TFSI remains not complexed to PPY. Thus in the other phase, the hygroscopic TFSI molecules are suggested to form phase separated water-rich domains upon water absorption, see Fig. 5 (right). It is known that TFSI and water molecules interact to form protonated water clusters [34], and Fig. 4 shows that lamellar self-assembly is observed with the periodicity of 11.31 Å (LS2 structure). We suggest that it is reminiscent of a lamellar liquid crystalline phase of water/surfactant mixtures, as driven by the amphiphilicity of TFSI [46]. Also in this case, the fluorines tend towards the film surface. As x is increased towards $x = 1.00$, the fraction of the liquid crystalline water/TFSI domains becomes dominant and the well defined LS1 structure of PPY complexes with TFSI becomes suppressed.

The above proposal would provide a natural explanation for the XRD and FT-IR data, and will be elaborated further in the context of wetting, polarised optical microscopy and electric transport. In qualitative agreement, Fig. 6 shows that PPY and PPY(TFSI)$_{0.25}$ have contact angles in the range of 57° and 45° as dried, and 37° and 35° after humidity treatment. But a step-wise change takes upon further adding TFSI, as for $x = 0.50$ the contact angles drop to near 10°. This coincides with the appearance of the LS2 structure, which we assign to the formation of phase separated water/TFSI domains. We expect that the latter domains promote wetting of water droplets. For higher x, a minor gradual increase of contact angle is observed. Polarised optical microscopy was of some help towards helping the assignment of the structures: Pure PPY is birefringent due to crystallisation. As dried, all the films PPY(TFSI)$_x$ are homogeneous at the resolution of optical microscopy. For small x, the humidity treatment caused minor birefringence, in agreement with the proposed self-assemblies (see Fig. 7a for the optical microscopy picture for PPY(TFSI)$_{0.25}$ after the humidity treatment). For the highest amount of TFSI ($x = 1.00$), even birefringent droplets were observed upon humidity treatment (see Fig. 7b: the noncomplexed TFSI caused high water absorption as droplets on the film surfaces and the TFSI/water interactions caused liquid crystalline-like birefringence in the droplets. Therefore, also polarised optical microscopy supports the suggestion shown in Fig. 5.

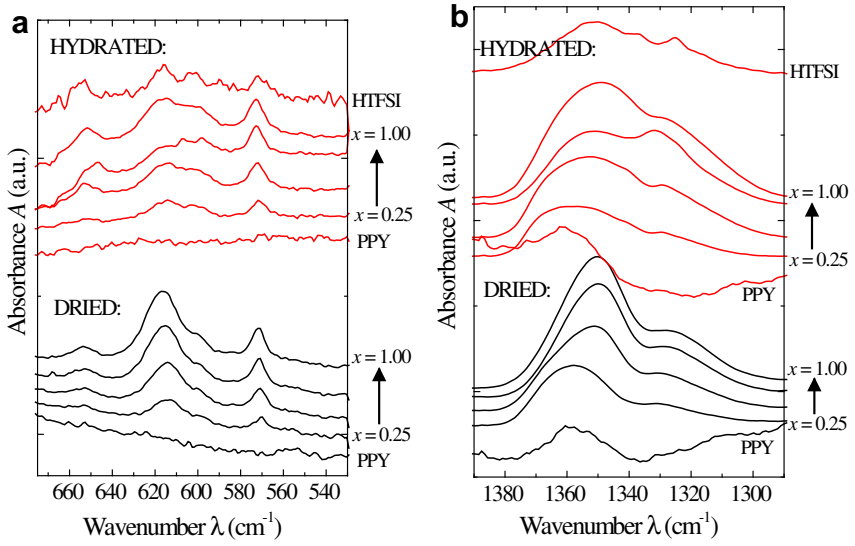

Fig. 9. FT-IR ATR spectra of PPY, TFSI and PPY(TFSI)$_x$ samples right after vacuum drying (black curves), and after a 150 h 80% RH water vapour treatment (red curves) for a) 670–530 cm^{-1} and b) 1390–1290 cm^{-1}. (For interpretation of the references to colour in this figure legend, the reader is referred to the web version of this article).

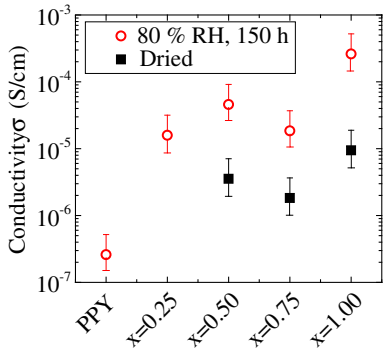

Fig. 10. Conductivity values of pure PPY and the PPY(TFSI)$_x$ complexes, all drop cast from formic acid solutions and dried in vacuum for two days (black squares) and treated in a humidity chamber at 80% RH/25 °C for 150 h (red circles). (For interpretation of the references to colour in this figure legend, the reader is referred to the web version of this article).

Finally, FT-IR ATR measurements reveal information on the conformation of TFSI within the PPY(TFSI) complexes in thin films. The $TFSI^-$ ion is known to adopt two different conformations: the cisoid form of C_1 symmetry and the transoid form of C_2 symmetry (see Fig. 8). The C_2 conformation has been reported to be more stable than the C_1 state by 2.3–3.3 kJ mol^{-1} [53–55]. The two states have qualitative differences in the FT-IR spectra of the SO_2 doublet band at ~ 1330/1350 cm^{-1}. The higher wavenumber component is more intense for the C_2 state than for the C_1 state and vice versa. There are also clear differences in the 500-680 cm^{-1} region: The component at ~ 620 cm^{-1} exists only due to the C_2 state and the two components near 602 and 656 cm^{-1} due to the C_1 state.

The FT-IR spectra of PPY(TFSI) thin films in Fig. 9a and b suggest that the conformation of the TFSI dopant indeed changes when moisture level increases in the films. In the dry state the higher wavenumber component of the doublet near 1350 cm^{-1} is more prominent with all complexes and the 602/656 cm^{-1} bands are weak, *i.e.* TFSI is mainly in the more stable C_2 state where it is likely to be trapped during the spin-coating process. As completely wet, all the characteristic bands for the C_1 component start to be more intense in the FT-IR spectra of all the complexes. However, the change is more evident when the fill factor increases and noteworthy, PPY(TFSI)$_{0.25}$ shows hardly any signs of the C_1 conformation. Thus we believe that the C_2 state is related to the PPY/TFSI lamellar self-assemblies (LS1/13 Å) and the C_1 state to the water/TFSI structure (LS2/11.3 Å), allowing to minimize the contact of the highly polar water and highly hydrophobic fluorines.

Conductivity values of drop cast PPY complexes were measured in the dry and hydrated state. Dry films were quite poorly conducting but after humidity treatment the resistance decreased in all of the complexes. The conductivity values of dry and wet samples are shown in Fig. 10. Pure PPY and PPY(TFSI)$_{0.25}$ were so poorly conducting in the dried state that the resistance values could not be measured with the available instrument. However, PPY(TFSI) in the hydrated state shows relatively high ionic conductivity of the order of 10^{-4} S/cm at its best at room atmosphere. Electronic conductivity indeed should not be possible, since PPY needs redox doping to be electronically conducting, which in addition is unstable under air [56,57]. Note that the films are bulk-like due to the drop casting technique and cannot thus show if the orientation has any effect on the conductivity.

4. Conclusions

Bis(trifluoromethane)sulfonimide (TFSI) is one of the strongest superacids and forms ionic liquids in acid–base complexes with several types of organic bases, as extensively studied for ionic liquids and electrochemical systems. Here we demonstrate well defined self-assemblies of acid-base complexes with a rod-like polymeric base poly(2,5-pyridine) upon a humidity treatment. The self-assembly results from the competition between the hydrophobic fluorine units in TFSI and the hydrophilic sulfonimide groups. The complexation leads to plasticisation, thus allowing the well defined self-assemblies upon water uptake. The PPY(TFSI) complexes show protonic conductivity, which is promoted by water uptake. Thus the concept suggests combining self-assemblies, rod-like polymers and ionic liquids to engineer materials for tailored proton transport and electrochemical devices.

Acknowledgements

We would like to thank Dr. Laszlo Almasy for his help with the preliminary X-ray studies and Dr. Antti Pelli for measuring the EDXRF spectra. Finnish Academy is acknowledged for financial support.

References

[1] Bao Z, Dodabalapur A, Lovinger AJ. Appl Phys Lett 1996;69:4108–10.
[2] Sirringhaus H, Brown PJ, Friend RH, Nielsen MM, Bechgaard K, Langeveld-Voss BMW, et al. Nature 1999;401:685–8.
[3] Dong H, Li H, Wang E, Yan S, Zhang J, Yang C, et al. J Phys Chem B 2009; 113:4176–80.
[4] McCulloch I, Heeney M, Bailey C, Genevicius K, MacDonald I, Shkunov M, et al. Nat Mater 2006;5:328–33.
[5] Ohtake T, Ogasawara M, Ito-Akita K, Nishina N, Ujiie S, Ohno H, et al. Chem Mater 2000;12:782–9.
[6] Kato T, Mizoshita N, Kishimoto K. Angew Chem Int Edition 2006;45:38–68.
[7] Scherer GG, editor. Adv Polym Sci. (Fuel cells I), vol. 215. Berlin/Heidelberg: Springer; 2008.
[8] Scherer GG, editor. Adv Polym Sci. (Fuel cells II), vol. 216. Berlin/Heidelberg: Springer; 2008.
[9] Li Q, He R, Jensen JO, Bjerrum NJ. Chem Mater 2003;15:4896–915.
[10] Ioselevich AS, Kornyshev AA, Steinke JHG. J Phys Chem B 2004;108:11953–63.
[11] Mauritz KA, Moore RB. Chem Rev 2004;104:4535–86.
[12] Eikerling M, Kornyshev AA, Spohr E. Adv Polym Sci 2008;215:15–54.
[13] Jiang SP, Liu Z, Tian ZQ. Adv Mater 2006;18:1068–72.
[14] Wiles KB, de Diego CM, de Abajo J, McGrath JE. J Membr Sci 2007;294:22–9.
[15] Chen W-F, Kuo P-L. Macromolecules 2007;40:1987–94.
[16] Jie Z, Haolin T, Mu P. J Membr Sci 2008;312:41–7.
[17] Gogel V, Jörissen L, Chromik A, Schönberger F, Lee J, Schäfer M, et al. Sep Sci Technol 2008;43:3955–80.
[18] Yu X, Roy A, Dunn S, Badami AS, Yang J, Good AS, et al. J Polym Sci A Polym Chem 2009;47:1038–51.
[19] Hu Z, Yin Y, Yaguchi K, Endo N, Higa M, Okamoto K. Polymer 2009;50: 2933–43.
[20] Saito T, Moore HD, Hickner MA. Macromolecules 2010;43:599–601.
[21] Ding J, Chuy C, Holdcroft S. Chem Mater 2001;13:2231–3.
[22] Norsten TB, Guiver MD, Murphy J, Astill T, Navessin T, Holdcroft S, et al. Adv Funct Mat 2006;16:1814–22.
[23] Rikukawa M, Sanui K. Progr Polym Sci 2000;25:1463–502.
[24] Armand M, Endres F, MacFarlane DR, Ohno H, Scrosati B. Nat Mater 2009;8:621–9.
[25] Nowinski JL, Lightfoot P, Bruce PG. J Mater Chem 1994;4:1579–80.
[26] Bonhôte P, Dias A-P, Papageorgiou N, Kalyanasundaram K, Grätzel M. Inorg Chem 1996;35:1168–78.
[27] Rey I, Johansson P, Lindgren J, Lassègues JC, Grondin J, Servant L. J Phys Chem A 1998;102:3249–58.
[28] Sun J, Forsyth M, MacFarlane DR. J Phys Chem B 1998;102:8858–64.
[29] MacFarlane DR, Meakin P, Sun J, Amini N, Forsyth M. J Phys Chem B 1999; 103:4164–70.
[30] Singh RP, Manandhar S, Shreeve JM. Tetrahedron Lett 2002;43:9497–9.
[31] Yoshizawa M, Xu W, Angell CA. J Am Chem Soc 2003;125:15411–9.
[32] Jin C-M, Shreeve JM. Inorg Chem 2004;43:7532–8.
[33] Matsumoto K, Hagiwara R. J Fluorine Chem 2007;128:317–31.
[34] Eikerling M, Paddison SJ, Zawodzinski Jr TA. J New Mat Electrochem Syst 2002;5:15–23.
[35] Noda A, Susan MdABH, Kudo K, Mitsushima S, Hayamizu K, Watanabe M. J Phys Chem B 2003;107:4024–33.
[36] Susan MdABH, Noda A, Mitsushima S, Watanabe M. Chem Commun; 2003: 938–9.
[37] Nakamoto H, Noda A, Hayamizu K, Hayashi S, Hamaguchi H, Watanabe M. J Phys Chem C 2007;111:1541–8.
[38] Marotta E, Rastrelli F, Saielli G. J Phys Chem B 2008;112:16566–74.
[39] Jia L, Nguyen D, Halleý JW, Pham P, Lamanna W, Hamrock S. J Electrochem Soc 2009;156:B136–51.

[40] Matsuoka H, Nakamoto H, Susan MdABH, Watanabe M. Electrochim Acta 2005;50:4015–21.
[41] Yang Z, Coutinho DH, Yang D-J, Balkus Jr KJ, Ferraris JP. J Membr Sci 2008; 313:91–6.
[42] Tigelaar DM, Waldecker JR, Peplowski KM, Kinder JD. Polymer 2006;47: 4269–75.
[43] Lodge TP. Science 2008;321:50–1.
[44] Simone PM, Lodge TP. ACS Appl Mater Interfaces 2009;1:2812–20.
[45] Virgili JM, Hexemer A, Pople JA, Balsara NP, Segalman RA. Macromolecules 2009;42:4604–13.
[46] Kato H, Nishikawa K, Koga Y. J Phys Chem B 2008;112:2655–60.
[47] Knaapila M, Ruokolainen J, Torkkeli M, Serimaa R, Horsburgh L, Monkman AP, et al. Synth Met 2001;121:1257–8.
[48] Knaapila M, Stepanyan R, Horsburgh LE, Monkman AP, Serimaa R, Ikkala O, et al. J Phys Chem B 2003;107:14199–203.
[49] Ikkala O, ten Brinke G. Chem Comm; 2004:2131–7.
[50] Smith P, Eisenberg A. Macromolecules 1994;27:545–52.
[51] Cesteros LC, Velada JL, Katime I. Polymer 1995;36:3183–9.
[52] Ruokolainen J, Torkkeli M, Serimaa R, Vahvaselkä S, Saariaho M, ten Brinke G, et al. Macromolecules 1996;29:6621–8.
[53] Johansson P, Gejji SP, Tegenfeldt J, Lindgren J. Electrochim Acta 1998;43: 1375–9.
[54] Herstedt M, Smirnov M, Johansson P, Chami M, Grondin J, Servant L, et al. J Raman Spectrosc 2005;36:762–70.
[55] Fujii K, Fujimori T, Takamuku T, Kanzaki R, Umebayashi Y, Ishiguro S. J Phys Chem B 2006;110:8179–83.
[56] Yamamoto T, Maruyama T, Zhou Z, Ito T, Fukuda T, Yoneda Y, et al. J Am Chem Soc 1994;116:4832–45.
[57] Yamamoto T, Nakamura T, Fukumoto H, Kubota K. Chem Lett 2001;30:502–3.